

# Differentiated Fractionation of Various Biomass Resources by *p*-Toluenesulfonic Acid at Mild Conditions

Shaohua Fang, Qiuli Xia, Lin Zhang,\* Peng Zhan, Yan Qing, Zhiping Wu, Hui Wang, Lishu Shao, Na Liu, Jiaying He, and Jin Liu



Cite This: *ACS Omega* 2023, 8, 24247–24255



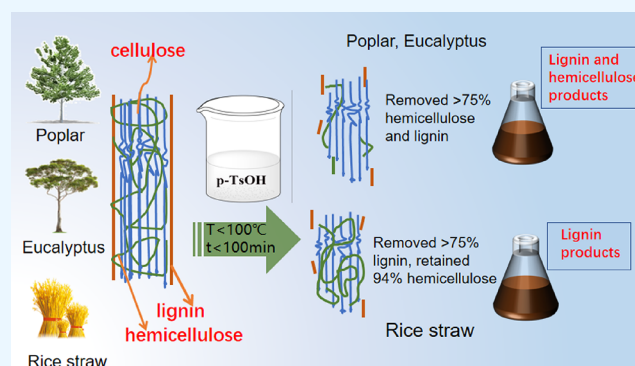
Read Online

ACCESS |

Metrics & More

Article Recommendations

**ABSTRACT:** Biomass is the ideal substitute for petrochemical resources because of its renewable and abundant sources. *p*-Toluenesulfonic acid (*p*-TsOH) can effectively separate lignin from biomass under mild conditions, so it is highly expected in biomass fractionation to improve the utilization efficiency. In this study, we investigated the effect of *p*-TsOH differentiated fractionation of poplar sawdust, eucalyptus sawdust, and rice straw below 100 °C. According to the experimental results, upon pretreatment by *p*-TsOH of the three kinds of raw biomass, most of the lignin and hemicellulose of poplar sawdust and eucalyptus sawdust were removed, whereas the cellulose was retained, but most of the hemicellulose and cellulose of rice straw were kept, whereas the lignin was removed at similar conditions. The structures and compositions of pretreatment residues, lignin, and hemicellulose extracted from raw biomass were characterized by XRD, FTIR, HSQC-NMR, XPS, and SEM. The differentiated fractionation mechanism of biomass was analyzed. A better recognition and understanding of the factors affecting biomatrix opening and fractionation will allow for the identification of new pretreatment strategies that improve biomass utilization and permit the rational enzymatic hydrolysis of cellulose.



## 1. INTRODUCTION

Biomasses are rich in carbohydrates and lignin, which can be used to produce biofuels and high-value-added chemicals. They are renewable, cheap, easy to obtain, etc. So, biomasses are an up-and-coming renewable resource. Improving the utilization efficiency of lignocellulose has positive significance for protecting the environment, promoting carbon neutralization, and establishing a circular economy.<sup>1</sup>

The structural complexity and component distribution heterogeneity of the plant cell wall constitute the natural antidegradation barrier in biomass transformation, which seriously hinders the efficient utilization of biomass fiber. Therefore, how to effectively break this structure, achieve the separation of lignin and hemicellulose, and try to avoid the deposition of separated lignin fragments on the substrate is a problem worth studying.<sup>2</sup> Especially, in the lignocellulose ethanol process, it is necessary to pretreat biomass materials before enzymatic hydrolysis to destroy the original structure of the plant cell wall, separate or remove some hemicellulose and lignin, reduce cellulose crystallinity, increase the porosity of the raw material substrate, and thus improve the accessibility of enzyme to cellulose to promote the conversion of cellulose and hemicellulose to monosaccharide.<sup>3</sup> One of the methods to

recover monosaccharides from cellulosic biomass is to isolate lignin, and the separation process is best performed in water systems given the consideration of solvent recovery costs and environmental issues.<sup>4</sup>

*p*-Toluenesulfonic acid (*p*-TsOH) has a hydrophilic sulfonic acid part and a hydrophobic toluene part, which is a good choice for water solvent. The  $\text{p}K_{\text{a}}$  of the aqueous *p*-TsOH solution is  $-2.8$ , which can easily provide hydrogen protons and break the chemical bond between lignin and carbohydrate (LCC).<sup>5</sup> Moreover, the benzene ring part of *p*-TsOH is a nonpolar oleophilic group, which can wrap lignin by  $\pi-\pi$  accumulation or hydrophobic formation, and it is conducive to the dissolution and separation of lignin.<sup>6</sup> Simultaneously, *p*-TsOH has a low solubility at room temperature. By cooling the concentrated waste acid solution to the ambient temperature and using the commercially proven crystallization technology,<sup>7</sup>

Received: February 12, 2023

Accepted: June 19, 2023

Published: June 29, 2023



*p*-TsOH can be recovered and recycled to achieve energy conservation, environmental protection, and sustainable development. The acid and water-assisted solubility of *p*-TsOH has the characteristic of the selective degradation of hemicellulose and lignin.<sup>8</sup> By dissolving the biomass fiber under appropriate conditions, the cellulose rich acid insoluble solids and the acid waste liquid, including dissolved lignin, can be obtained. So, *p*-TsOH is widely used in organic acid treatment, which is due to the strong electron absorption characteristics of the aromatic ring of *p*-TsOH, enhanced ionization capacity of hydrogen ions, and good water absorption and recyclability.<sup>7</sup> Mild condition *p*-TsOH treatment at high concentrations has been shown to effectively remove lignin.<sup>9</sup>

Chen et al.<sup>1</sup> found that *p*-TsOH was characterized by selective delignification at 80% concentration, Feng et al.<sup>7</sup> proved that *p*-TsOH treatment could effectively remove lignin under mild conditions, and Yang et al.<sup>10</sup> used *p*-TsOH to remove lignin and xylose and explored the saccharification rate of solid residues after pretreatment. Currently, studies on *p*-TsOH water treatment focus on optimizing the pretreatment parameters, separation mechanism, and substrate conversion to achieve efficient lignin extraction. No systematic and comprehensive research has been conducted based on different types of biomass raw materials, lignin, and hemicellulose structural components to explore the effect of *p*-TsOH aqueous solution pretreatment on different types of biomasses. It is a relatively new research direction whether the pretreatment effect of *p*-TsOH on woody and herbaceous biomass is consistent. Various plant fiber raw material contents, compositions, and structures are not the same; the same plant fiber raw material generally will have a variety of formats. Here, we selected three biomass raw materials, poplar, eucalyptus, and rice straw, for pretreatment and analysis of the results. Poplar is the most widely planted, fast growing tree species in the world, and it is an essential raw material for the bioenergy industry.<sup>11</sup> Eucalyptus is a broad-leaved wood with a chemical composition close to poplar, which has a fast growth cycle and a long average fiber length, and it is also an ideal biomass raw material.<sup>12</sup> As a representative plant of herbaceous biomass raw materials, rice straw has a different composition from the two wood fiber raw materials, poplar and eucalyptus.<sup>13</sup> For the pretreatment process of these three biomass raw materials, the differentiation in the separation and extraction process triggered our thinking.<sup>14</sup>

In this study, we discussed the effect of the concentration of *p*-TsOH aqueous solution, temperature, and time on the pretreatment impact on poplar, eucalyptus, and rice straw, and the effect on the enzymatic hydrolysis efficiency. At the same time, we found that *p*-TsOH greatly differed in the degradation effects on hemicellulose of poplar, eucalyptus, and rice straw. Combined with the structural composition and dissolution mechanism of hemicellulose and lignin for the three kinds of biomass, it provides a valuable theoretical basis for the reason for the differentiated degradation of woody biomass and herbal biomass.

## 2. MATERIALS AND METHODS

**2.1. Materials.** Poplar sawdust, eucalyptus sawdust, and rice straw were respectively obtained from Shandong, Guangxi, and Jiangxi province, China. The chemical composition was detected according to the National Renewable Energy Laboratory (NERL) standard method,<sup>15</sup> and results are

shown in Table 1. *p*-Toluenesulfonic acid and other chemical reagents were purchased from Aladdin Biochemical Technology (Shanghai, China).

**Table 1. Compositions of the Three Kinds of Biomass**

sample	cellulose/%	hemicellulose/%	lignin/%	ash/%
poplar sawdust	46.13	17.31	26.19	0.30
eucalyptus sawdust	42.38	15.78	26.79	1.16
rice straw	34.34	17.97	27.85	9.67

**2.2. Pretreatment of Biomass.** **2.2.1. Pretreatment Methods.** The three kinds of biomass were reacted by *p*-TsOH treatment. We referred to the studies of Chen et al.,<sup>1</sup> Zhu et al.,<sup>16</sup> and Duan et al.<sup>17</sup> to determine the range of acid concentrations used for pretreatment. Biomass (5 g) was added to the conical flask and mixed into a *p*-TsOH solution. The solid–liquid ratio was 1:10 (w: v), and the mixture was heated in a high-temperature shaker (JIEXING, TS-200A, China). The reaction was carried out at different *p*-TsOH concentrations, temperatures, and times. The reaction was terminated by injecting cold deionized water (80 mL) into the response system. The residue and pretreatment solution were separated by suction filtration. The residue was washed with water and ethanol.

**2.2.2. Analysis Methods.** The compositional analysis of all the pretreated residue and raw materials was also performed by the NREL method. Quantitative glucose and xylose in hydrolysate were determined using a high-performance liquid chromatography system (HPLC, Shodex LC-16, Japan). The velocity of the mobile phase in the HPLC analysis system was 0.6 mL min<sup>-1</sup>, and the temperature was 45 °C.<sup>18</sup> The acid-soluble lignin was measured by a UV spectrophotometer (YOKE, T2600, China) at a wavelength of 320 nm. The morphologies of the pretreated residue and raw materials were characterized by scanning electron microscopy (SEM, TESCAN, Czech Republic). The methods and processes were as described by Majumdar et al.<sup>19</sup> The crystallinity of the three raw materials was detected by an X-ray diffraction instrument (XRD, Bruker D8 Advance, Germany).<sup>20</sup>

**2.3. Enzymatic Hydrolysis of the Pretreated Residue of Biomass.** Enzymatic hydrolysis reactions were performed to test the effect of the pretreatment. Pretreated residue (1 g) was put into the cone flask, and 50 mL sodium citrate buffer solution and then enzymes were added. We used cellulase and  $\beta$ -glucosidase for enzymatic digestion. The amounts of cellulase and  $\beta$ -glucosidase used were 15 and 9.375 U g<sup>-1</sup>. The amount of cellulase was studied in Yang et al.<sup>10</sup> The cellulase was provided by KDN Biotechnology (Shandong, China). The cellulase activity was 128.5 FPU/mL (fiber filter paper activity unit), as calibrated by a method in the literature.<sup>21</sup> The  $\beta$ -glucosidase activity was 20 FPU/mL as provided by Xiasheng Biotechnology (Ningxia, China). Then, the cone flasks were put into the shaker, and the shaker temperature of 50 °C was set at 180 rpm for 72 h. After the reaction, the boiling water bath was used for 10 min and cooled to room temperature, and the hydrolysates and residues were separated by a syringe. The sugar content of the hydrolysates was determined by high-performance liquid chromatography (HPLC, SHODEX LC-16, Japan).<sup>22</sup>

**2.4. Hemicellulose Extraction and Analysis.** **2.4.1. Hemicellulose Extraction from Biomass.** Ten grams of biomass was mixed with 100 mL of 5% NaOH aqueous solution at a

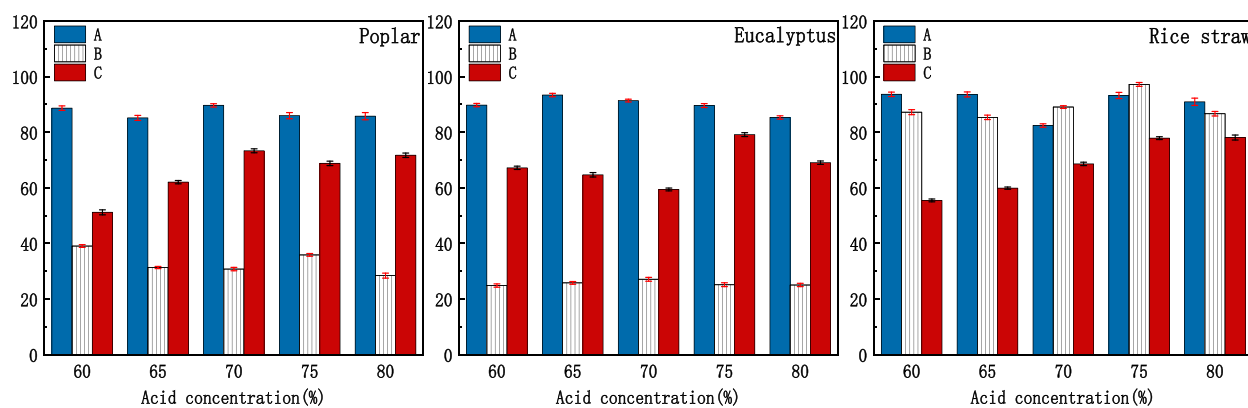


**Figure 1.** Effect of pretreatment on three biomasses by different concentrations of *p*-TsOH ((A) retention rate of cellulose (%), (B) retention rate of hemicellulose (%), and (C) removal rate of lignin (%)).

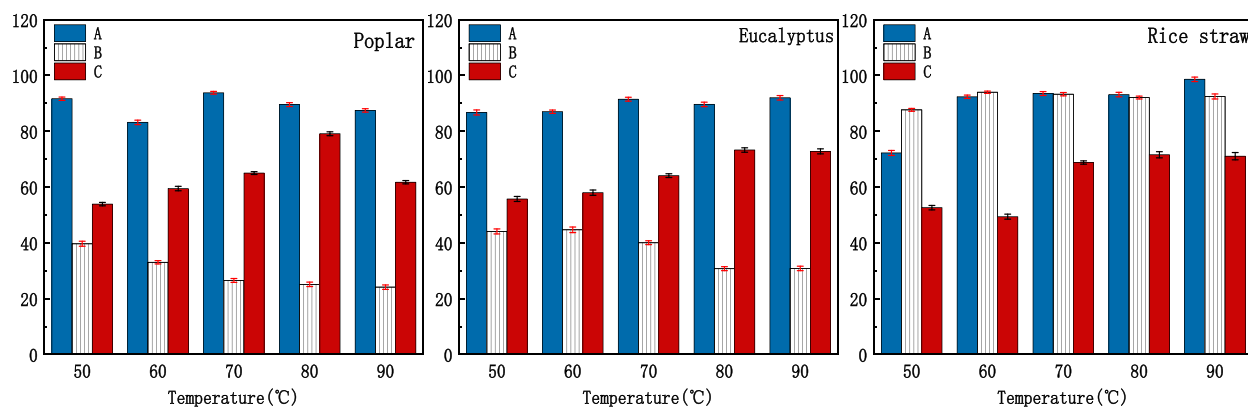


**Figure 2.** Effect of pretreatment on three biomasses by different temperatures ((A) retention rate of cellulose (%), (B) retention rate of hemicellulose (%), and (C) removal rate of lignin (%)).

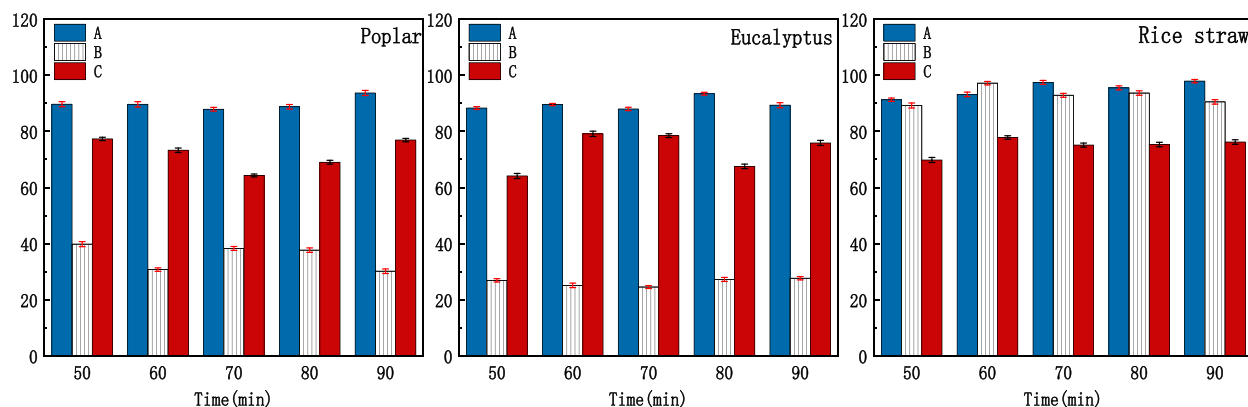


**Figure 3.** Effect of pretreatment on three biomasses by different times ((A) retention rate of cellulose (%), (B) retention rate of hemicellulose (%), and (C) removal rate of lignin (%)).

conical flask, which was placed in a high-temperature shaker. The temperature of the high-temperature shaker was set to 80 °C, and the running time was 80 min. After the reaction, 900 mL of deionized water was put into the reaction liquid, and then added 6000 mL ethanol stranded for 24 h.<sup>23</sup> The hemicellulose precipitation was then collected. The dry hemicellulose was obtained by centrifugation for 20 min using a freeze dryer dried for 24 h.

**2.4.2. Analysis Methods of Hemicellulose.** The hemicelluloses obtained were subjected to Fourier transform infrared spectroscopy (FTIR) analysis. The infrared spectra were acquired using a Thermo Scientific Nicolet 7600 FTIR

spectrometer over a frequency range between 4000 and 400  $\text{cm}^{-1}$ .<sup>24</sup> The surface chemistry of extracted hemicellulose of the three kinds of biomass was analyzed by X-ray photoelectron spectroscopy (XPS, Thermo Scientific K-Alpha) with a vacuum of  $2 \times 10^{-10}$  mbar. The 2D-NMR (HSQC) spectra of the hemicelluloses were acquired at 25 °C on a Bruker AVIII 400 MHz spectrometer (Bruker, Germany).<sup>25</sup> Elemental analysis of hemicelluloses was performed on a CHNS elemental analyzer (ELEMENTAR Vario ELIII, Germany).<sup>26</sup>

**2.5. Lignin Extraction and Analysis.** **2.5.1. Lignin Extraction from the Supernatant Fluid of Pretreatment.** After the pretreatment, the pretreatment liquid was collected,

added 6 times volume of deionized water, and left to stand for 24 h, and then lignin was collected by centrifugation for 20 min and using the freeze dryer dried for 24 h.<sup>27</sup>

**2.5.2. Analysis Method of Lignin.** The lignin obtained was subjected to Fourier transform infrared spectroscopy (FTIR) analysis. The infrared spectra were acquired using a Thermo Scientific Nicolet 7600 FTIR spectrometer over a frequency range between 4000 and 400  $\text{cm}^{-1}$ .<sup>24</sup> The 2D-NMR (HSQC) spectra of the hemicelluloses were acquired at 25 °C on a Bruker AVIII 400 MHz spectrometer (Bruker, Germany).<sup>25</sup> The integrations of the peaks in the  $^{13}\text{C}$ - $^1\text{H}$  spectrum and contours in 2D-NMR plots were conducted using the MestReNova software. The detailed calculation method was based on the modified method from previous literature.<sup>6,28</sup>

### 3. RESULTS AND DISCUSSION

#### 3.1. Solid Yields and Their Compositional Analysis.

**3.1.1. Analysis of the Univariate Experiments.** The effect of *p*-TsOH concentration, temperature, and reaction time on the pretreatment was studied. As shown in Figure 1, upon increasing *p*-TsOH concentration from 60 to 80%, lignin dissolution of poplar was highest at 70%, and the removal rate of lignin reached 73.3%; for eucalyptus and rice straw, lignin dissolution was highest at 75%, and the removal rate reached 79.13 and 77.85%, respectively, after 60 min fractionation at 80 °C. Similarly, upon increasing temperature from 50 to 90 °C, lignin dissolutions of poplar, eucalyptus, and rice straw were highest at 80 °C after 60 min reaction at a *p*-TsOH concentration of 70% (Figure 2). Upon increasing time from 50 to 90 min, lignin dissolutions of poplar and rice straw were highest at 90 min and that of eucalyptus was highest at 70 min after fractionation at 80 °C reaction at a *p*-TsOH concentration of 70% (Figure 3). Under mild conditions, *p*-TsOH pretreatment showed a high lignin removal rate.

Whereas most of the lignin was dissolved into the *p*-TsOH solution, the hemicellulose had different results from the three kinds of biomass. For the woody biomasses poplar sawdust and eucalyptus sawdust, the hemicellulose could be removed whereas cellulose was kept, and the retention rate of hemicellulose reached 28.39 and 24.53%, respectively. But for the herbaceous biomass rice straw, most cellulose and hemicellulose were retained, and the retention rate of hemicellulose reached 94.01%. Ma et al.<sup>14</sup> used 50% *p*-TsOH to pretreat rice straw; while under 90–100 °C for 0–360 min, the loss ratio of hemicellulose was up to 80%. Compared to our research, they conducted a higher temperature and extended time with a lower *p*-TsOH content, so there was a different result of the removal rate of hemicellulose. Meanwhile, most of the retention rates of cellulose were up to 90% after the *p*-TsOH pretreatment (Figures 1–3).

**3.1.2. XRD and SEM.** The pretreatment process generally changes the crystallinity of the fiber, which affects the hydrolytic efficiency of the cellulose. The XRDs for without pretreatment and with *p*-TsOH of the three kinds of biomass were analyzed as shown in Figure 4. At the positions of 15.8, 22.5, and 34.9, all the samples showed characteristic peaks typical of the cellulose type I structure. Compared with the raw material, the pretreatment sample residue was sharper at position 22.5, and the peak intensity was significantly strengthened. In addition, as seen in Figure 4, no additional peaks appeared, indicating that the original structure of cellulose was not destroyed.

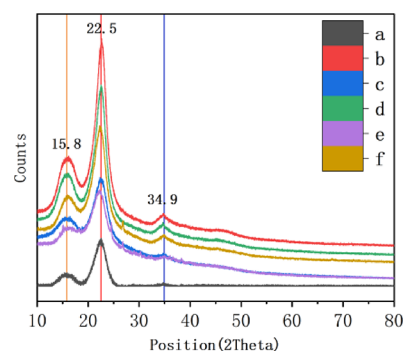


**Figure 4.** XRD analysis of the three kinds of biomass before and after pretreatment ((a) poplar sawdust, (b) pretreated poplar sawdust, (c) eucalyptus sawdust, (d) pretreated eucalyptus sawdust, (e) rice straw, and (f) pretreated rice straw).

Meanwhile, we analyzed crystallinity changes of poplar sawdust, eucalyptus sawdust, and rice straw before and after pretreatment (Table 2). The significant increase in crystallinity

**Table 2. Results for Change of Crystallization**

sample	untreated	pretreated	increase in value
poplar	39.73%	76.59%	93%
eucalyptus	43.14%	66.99%	55%
rice straw	41.41%	57.45%	39%

was attributed to the pretreatment for the removal of large amounts of lignin, hemicellulose, as well as amorphous cellulose, exposing more internal cellulose.

The surface of the three kinds of biomass became rougher after pretreatment, as shown in Figure 5. The character of the

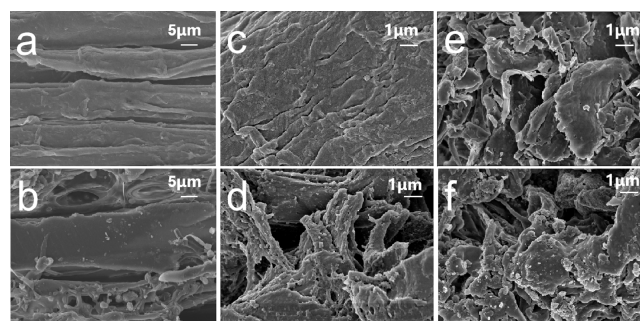


**Figure 5.** SEM pictures of the three kinds of biomass before and after *p*-TsOH pretreatment ((a) poplar sawdust, (b) pretreated poplar sawdust, (c) eucalyptus sawdust, (d) pretreated eucalyptus sawdust, (e) rice straw, and (f) pretreated rice straw).

untreated biomass had a tight structure, but the pretreated residue became wrinkled, grooved, and cracked. The results proved that the pretreatment of *p*-TsOH acid destroyed the form of poplar sawdust, eucalyptus sawdust, and rice straw.

#### 3.1.3. Enzymatic Enzyme Saccharification Results.

$$\text{SR} = \frac{\text{C}_0}{\text{C}_1 \div 0.9} \times 100\%$$

The results of enzymatic saccharification are shown in Table 3. The saccharification rate of rice straw, 86.99%, was higher than those of poplar sawdust and eucalyptus sawdust. The sugar recovery rate of rice straw, 77.00%, was far above those of poplar sawdust and eucalyptus sawdust, which were 55.56

Table 3. Results of Enzymatic Hydrolysis<sup>a</sup>

sample	cellulose			hemicellulose			enzymatic hydrolysis			
	Unt/g	Pret/g	RR/%	Unt/g	Pret/g	RR/%	Glu/g	Xyl/g	SR/%	SRR/%
poplar	0.4613	0.6880	89.65%	0.1731	0.0911	30.75%	0.56	0.032	73.30	55.56
eucalyptus	0.4238	0.7548	89.58%	0.1578	0.0756	25.13%	0.48	0.028	57.23	44.84
rice straw	0.3434	0.6414	93.20%	0.1797	0.2135	92.11%	0.62	0.066	86.99	77.00

<sup>a</sup>Pretreatment conditions: poplar, P 70% T 80 °C t 90 min; eucalyptus, P 75% T 80 °C t 80 min; rice straw, P 75% T 80 °C t 90 min. Unt: untreated, Pret: pretreatment, RR: retention rate, Glu: glucose, Xyl: xylose, SR: saccharification rate, SRR: saccharification recycle rate, C0: Glu, C1: pretreatment of cellulose.

and 44.84%, respectively. So, the rice straw treated by *p*-TsOH is an ideal resource for the lignocellulose ethanol process.

### 3.2. Analysis of the Hemicellulose Extraction.

**3.2.1. FTIR.** FTIR was used to analyze the differentiation of the three hemicellulose structures of hemicellulose extraction from the three kinds of biomass. Results of the analysis are shown in Figure 6. The broad peak at 3390 cm<sup>-1</sup> and the

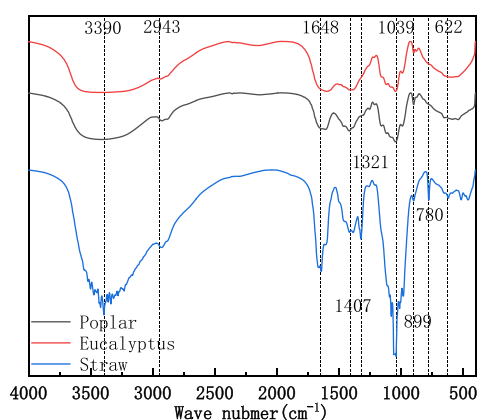


Figure 6. FTIR analysis of hemicellulose.

characteristic peaks at 1407 cm<sup>-1</sup> represent the expansion and vibration of the hydroxyl structure (-OH),<sup>29</sup> in which the distinct peaks of rice straw hemicellulose at 3390 cm<sup>-1</sup> are higher than those of poplar sawdust and eucalyptus sawdust, indicating more free hydroxyl structures. A rich hydroxyl structure (-OH) can be hyperbranched. Different functional groups can be introduced to obtain unique properties such as hydrophobicity, thermoelectric, water solubility, surface activity, biological functionality, conductivity, and stimulus responsiveness.<sup>30</sup>

The characteristic absorption peak at 2943 cm<sup>-1</sup> originates from the C-H symmetric or asymmetric telescopic vibration of the methyl/methylene groups, representing the vibration of the  $\beta$ -glycosidic bonds between the various sugar units, further indicating that this hemicellulose powder contains more sugar unit.<sup>31</sup> The absorption peak at 1648 cm<sup>-1</sup> belongs to the skeletal aroma (C-C) of lignin.<sup>32</sup> The spectra also show the characteristic peaks related to the syringyl Lignin (S) structures (at 1321 cm<sup>-1</sup>),<sup>26</sup> indicating that parts of the cellulose and lignin remain in the extracted hemicellulose. The absorption

peak at 1039 cm<sup>-1</sup> is due to the expansion vibration of xylose C-O and C-C or the bending pulse of C-OH of poly-xylose, the characteristic absorption peak of xylose,<sup>33</sup> which is higher in the hemicellulose of rice straw. The absorption peaks at 899 and 622 cm<sup>-1</sup> are attributed to the C-H deformation in the attached  $\beta$ -1-4 glycosidic bond.<sup>34</sup> The figure shows that the content of this structure is more in the hemicellulose of rice straw than poplar sawdust and eucalyptus sawdust. This was a typical  $\beta$ -heterodimer structure. The absorption peak at 780 cm<sup>-1</sup> is attributed to the C-H deformation in the attached  $\beta$ -1-4 glycoside bond, which is typical of the  $\beta$ -heterodimer structure.<sup>35</sup> This characteristic peak was evident in the hemicellulose of rice straw, which indicated that the hemicellulose of rice straw had more  $\beta$ -1-4 glycoside than the hemicellulose of poplar sawdust and eucalyptus sawdust.

**3.2.2. EA.** Comprehensive analysis of element results (Table 4) shows that the value of O/C in the hemicellulose of rice straw is much higher than the hemicellulose of poplar sawdust and eucalyptus sawdust. According to the elemental analysis of three hemicellulose chemical compositions and oxygen-carbon ratios in the hemicellulose, the O and H atoms of the hemicellulose of rice straw are more than the number of C atoms. Combined with the analysis of FTIR (3390 cm<sup>-1</sup>), we come to the conclusion that the hemicellulose of rice straw has more hydroxyl structures (-OH).

**3.2.3. 2D-HSQC NMR.** The structural features of the polysaccharides were analyzed using NMR.<sup>36</sup> According to 2D-HSQC spectroscopy (Figure 7), the semiquantitative analysis was performed (Table 5), which referenced the literature.<sup>37</sup> For example, in the hemicellulose of poplar sawdust, the content of (1-4)- $\beta$ -D-xylose (X) is 64.8%, and that of 4-O-Me- $\alpha$ -D-GlcpA (U) in the side chain is 20.7%. The content of  $\alpha$ -L-arabinose (Ara) is 17.5%. In the hemicellulose of eucalyptus sawdust, the content of (1-4)- $\beta$ -D-xylose (X) is 63.36%, and that of 4-O-Me- $\alpha$ -D-GlcpA (U) in the side chain is 18.8%. The content of  $\alpha$ -L-arabinose (Ara) is 16.9%. The content of (1-4)- $\beta$ -D-xylose(X) is 73.0% in the hemicellulose of rice straw, with no side chain structure. Meanwhile, according to the 2D-HSQC spectrum (Figure 7), LCC was found in the hemicellulose samples. PCA and FA (*p*-hydroxycinnamates) were 2.9 and 3.6%, respectively, in models of poplar and eucalyptus. In the hemicellulose of rice straw, the A<sub>γ</sub> and A<sub>β(G/H)</sub> shared 21.7%.<sup>8,38</sup>

Table 4. Elementary Analysis of Hemicellulose of the Three Kinds of Biomass

sample	C (%)	H (%)	O (%)	N (%)	S (%)	O/C	H/O	chemical formula
poplar	32.06	5.65	47.58	0.14	0.04	1.1131	1.9000	C <sub>5</sub> H <sub>10.58</sub> O <sub>5.56</sub>
eucalyptus	28.78	4.42	46.78	0.13	0.24	1.2425	1.4832	C <sub>5</sub> H <sub>8.51</sub> O <sub>6.13</sub>
rice straw	24.3	4.78	41.94	0.24	0.17	1.2944	1.8236	C <sub>5</sub> H <sub>11.58</sub> O <sub>6.47</sub>

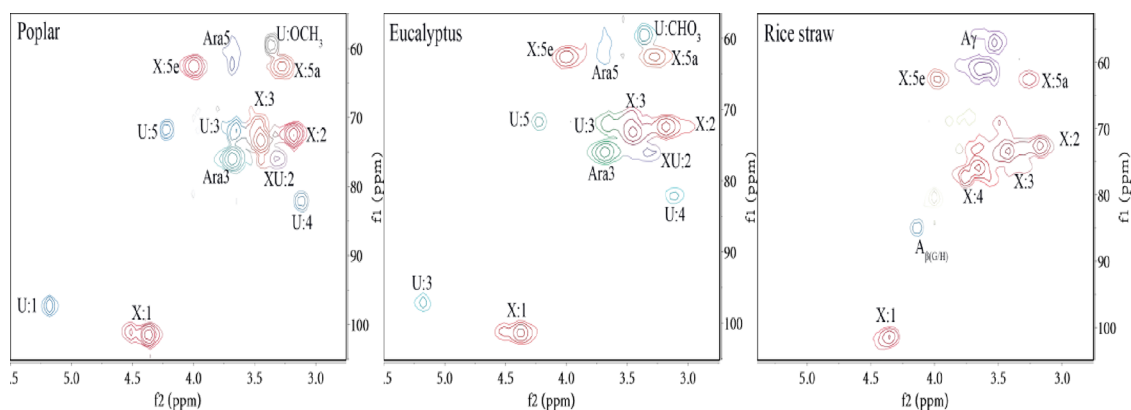


**Figure 7.** 2D-HSQC NMR of hemicellulose (X: (1-4)- $\beta$ -D-xylose, U: 4-O-Me- $\alpha$ -D-GlcP, XU: PCA and FA (*p*-hydroxycinnamates), Ara:  $\alpha$ -L-arabinose, A $\gamma$ : C $\gamma$ -H $\gamma$  in  $\gamma$ -acetylated  $\beta$ -O-4 substructures, A $\beta$ (G/H): C $\beta$ -H $\beta$  in  $\beta$ -O-4 substructures linked to G and H units).

**Table 5.** The Content of Structures in the Hemicellulose of Poplar Sawdust, Eucalyptus Sawdust, and Rice Straw

sample	poplar	eucalyptus	rice straw
X:1/%	13.2	13.26	8.3
X:2/%	14.7	14.1	11.3
X:3/%	20.1	20.9	20.1
X:4/%	0	0	25.2
X:5/%	0	0	0.21
X:5a/%	8.4	6.9	3.5
X:5e/%	8.4	8.6	4.4
XU:2/%	2.9	3.6	0
U:1/%	2.5	2.2	0
U:1/%	2.5	2.2	0
U:3/%	4.7	2.9	0
U:4/%	2.1	2.1	0
U:5/%	2.3	2.0	0
U:OCH <sub>3</sub> /%	4.4	6.7	0
Ara3/%	15.2	14.7	0
Ara5/%	2.3	2.2	0
A $\gamma$ /%	0	0	19.5
A $\beta$ (G/H)/%	0	0	2.2

The hemicellulose of the three kinds of biomass is mainly xylose. The backbone is (1-4)- $\beta$ -D-xylose (X) in the hemicellulose of poplar sawdust and eucalyptus sawdust, and  $\alpha$ -L-arabinose and 4-O-Me- $\alpha$ -D-GlcP (U) served as a branch. The backbone is (1-4)- $\beta$ -D-xylose (X) in the hemicellulose of rice

straw, without branching chains. It can also be verified in the analysis of FTIR that the  $\beta$ -1-4 glycoside of the hemicellulose of rice straw was higher than the two kinds of woody biomass. This less branched structure of the hemicellulose in rice straw makes the structure not susceptible to be broken and separated by *p*-TsOH.<sup>39</sup>

**3.3. Analysis of Lignin.** 3.3.1. *FTIR.* The FTIR results of lignin from the pretreatment liquid are shown in Figure 8. All the samples showed the typical lignin structure spectrum: hydroxyl (–OH) extension vibration at 3384 cm<sup>–1</sup> and C–H bonds in methyl and methyl side chains at 2939 and 2835 cm<sup>–1</sup>. The C=O expansion vibration at 1424–1514 cm<sup>–1</sup> is the aromatic ring skeleton vibration, representing the primary structure of lignin, C–O–C expansion vibration at 1220 cm<sup>–1</sup>, and C–O vibration of P syringe base at 1327 cm<sup>–1</sup>. The C–H substitutions at 841 and 770 cm<sup>–1</sup> show strong absorption, including 1608, 1460, 1327, and 1123 cm<sup>–1</sup>, the most. The C–O–C asymmetric vibration at 1152 and 1030 cm<sup>–1</sup> is the aromatic ring deformation and vibration in the C–H surface, representing the wood foundation (G) structure, C=O expansion vibration at rice straw lignin at 1653 cm<sup>–1</sup>, and a P syringe foundation absorption at 841 cm<sup>–1</sup>. In all three lignins, S unit lignin and G unit lignin were present.<sup>40</sup>

3.3.2. *2D-HSQC NMR.* We used 2D-HSQC NMR spectroscopy to analyze the dissolved lignin parts of the three kinds of biomass under the same treatment conditions. Figure 9 shows the four NMR spectra describing the side chains and aromatic regions, along with the determined chemical structures. Table

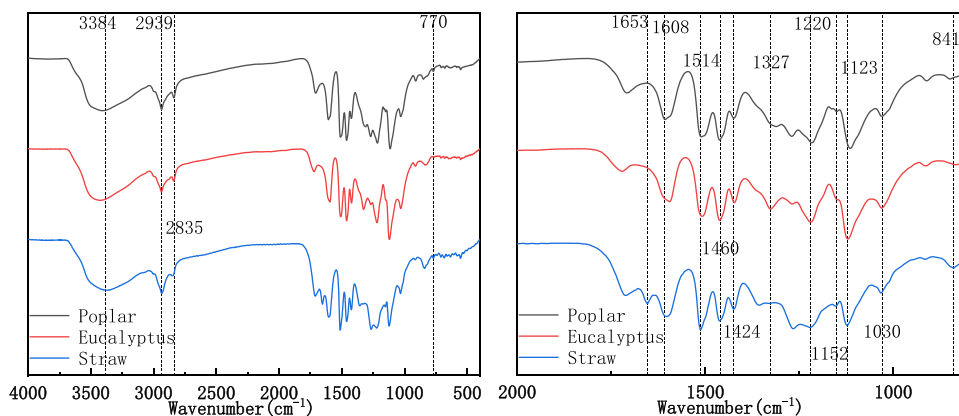


**Figure 8.** FTIR analysis of lignin.

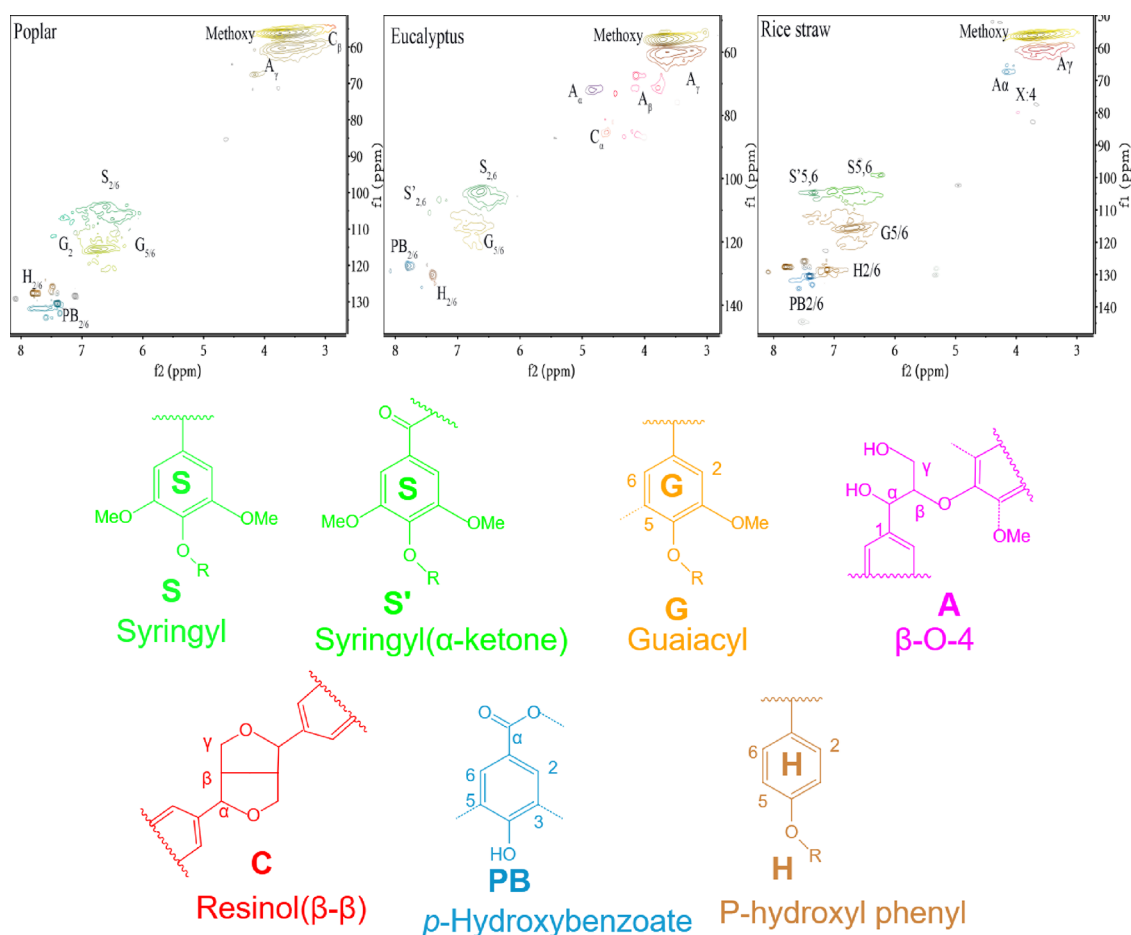


**Figure 9.** Fragrant and side chain region ( $\delta C/\delta H$  50–140/2.5–8.0) in the 2D HSQC NMR spectra of lignin samples of poplar sawdust, eucalyptus sawdust, and rice straw; the structural maps of lignin.

**Table 6.** Structural Features of the Dissolved Lignin Obtained from the  $^1\text{H}$ - $^{13}\text{C}$  Related Peak Integration in the HSQC Spectra

sample	S/%	G/%	$\beta$ -O-4/%	$\beta$ - $\beta$ /%	<i>p</i> -hydroxybenzoates/%	S/G	S/(G + H)
poplar	59.65	23.10	3.71	0	22.36	2.58	1.31
eucalyptus	67.02	28.19	14.46	2.57	15.32	2.37	1.54
rice straw	60.92	33.87	2.98	0	23.42	1.80	1.06

6 shows  $^1\text{H}$ - $^{13}\text{C}$  profile integration data for lignin structures that are listed in detail. The spectrum (Figure 9) shows that the dissolved lignin from the three kinds of biomass was composed mainly of syringyl (S), guaiacyl (G), and *p*-hydroxybenzoates (PB). Structural maps of these lignins are shown in the lower half of Figure 9. The lignin of rice straw contains relatively higher hydroxybenzoate (H) units, and the syringyl-to-guaiacyl (S/G) ratio is relatively low.

The C-5 position of the guaiacyl (G) lignin benzene ring is in a free state and can form a stable C–C bond by cross-linking with other C groups. The C-5 position of the syringyl (S) lignin benzene ring is the methoxy group, which cannot form a C–C bond. The connection is relatively loose. Compared with guaiacyl (G) lignin, syringyl (S) lignin is more likely to be degraded. The ratio of syringyl-to-guaiacyl (S/G) can reflect the difficulty of lignin removal; the higher the ratio is, the more easily lignin is removed for the less methoxy group content.<sup>41</sup> In rice straw lignin, the H lignin content is relatively high; this coincides with the difference between woody and herbaceous biomass raw materials, and the ratio of syringyl to guaiacyl (S/G) and ratio of syringyl to guaiacyl plus hydroxybenzoate (S/

(G + H)) are relatively low (Table 6), so the lignin of rice straw in *p*-TsOH pretreatment is more difficult to remove than poplar sawdust and eucalyptus sawdust lignin. At the same time, in the lignin of rice straw, some lignin carbohydrate complex (LCC) was found, and the LCC acts as an inhibitor in hot water to hemicellulose extraction, which was consistent with the results of hemicellulose 2D-NMR analysis.<sup>30</sup>

#### 4. CONCLUSIONS

In this study, we explored the pretreatment of poplar sawdust, eucalyptus sawdust, and rice straw by the *p*-TsOH process at mild conditions. The study showed a difference in the fractionation of the three types of biomasses. On the basis of the analysis of hemicellulose extracted from the three kinds of biomass, it can be concluded that the pretreatment of *p*-toluenesulfonic is an effective method to remove lignin and hemicellulose from woody biomasses such as poplar sawdust and eucalyptus sawdust. For herbaceous biomasses such as rice straw, the pretreatment of *p*-toluenesulfonic can remove lignin but retain large amounts of cellulose and hemicellulose. The main reason is that rice straw hemicellulose, which contains

many more free hydroxyl structures (–OH) and whose backbone lacks branches, is different from poplar sawdust and eucalyptus sawdust. Its hemicellulose structure is not susceptible to being broken by *p*-TsOH. After a comparative study, the pretreatment by *p*-TsOH has excellent potential in the biomass refining industry, especially producing bioethanol based on rice straw resource and functional fiber based on poplar and eucalyptus resource. Meanwhile, because of the easy recovery and recycling characteristics of *p*-TsOH, its role in sustainable economy and carbon footprint reduction will further be highlighted.

## AUTHOR INFORMATION

### Corresponding Author

**Lin Zhang** – College of Materials Science and Engineering, Ministry of Forestry Bioethanol Research Center, and Hunan International Joint Laboratory of Woody Biomass Conversion, Central South University of Forestry and Technology, Changsha 410004, China; [orcid.org/0000-0002-0481-4357](https://orcid.org/0000-0002-0481-4357); Email: [zhlin-331@163.com](mailto:zhlin-331@163.com)

### Authors

**Shaohua Fang** – College of Materials Science and Engineering, Ministry of Forestry Bioethanol Research Center, and Hunan International Joint Laboratory of Woody Biomass Conversion, Central South University of Forestry and Technology, Changsha 410004, China; [orcid.org/0000-0003-4019-8229](https://orcid.org/0000-0003-4019-8229)

**Qiuli Xia** – College of Materials Science and Engineering, Ministry of Forestry Bioethanol Research Center, and Hunan International Joint Laboratory of Woody Biomass Conversion, Central South University of Forestry and Technology, Changsha 410004, China

**Peng Zhan** – College of Materials Science and Engineering, Ministry of Forestry Bioethanol Research Center, and Hunan International Joint Laboratory of Woody Biomass Conversion, Central South University of Forestry and Technology, Changsha 410004, China

**Yan Qing** – College of Materials Science and Engineering, Ministry of Forestry Bioethanol Research Center, and Hunan International Joint Laboratory of Woody Biomass Conversion, Central South University of Forestry and Technology, Changsha 410004, China; [orcid.org/0000-0003-3260-7838](https://orcid.org/0000-0003-3260-7838)

**Zhiping Wu** – College of Materials Science and Engineering, Ministry of Forestry Bioethanol Research Center, and Hunan International Joint Laboratory of Woody Biomass Conversion, Central South University of Forestry and Technology, Changsha 410004, China; [orcid.org/0000-0001-8022-4837](https://orcid.org/0000-0001-8022-4837)

**Hui Wang** – College of Materials Science and Engineering, Ministry of Forestry Bioethanol Research Center, and Hunan International Joint Laboratory of Woody Biomass Conversion, Central South University of Forestry and Technology, Changsha 410004, China

**Lishu Shao** – College of Materials Science and Engineering, Ministry of Forestry Bioethanol Research Center, and Hunan International Joint Laboratory of Woody Biomass Conversion, Central South University of Forestry and Technology, Changsha 410004, China

**Na Liu** – College of Materials Science and Engineering, Ministry of Forestry Bioethanol Research Center, and Hunan International Joint Laboratory of Woody Biomass

Conversion, Central South University of Forestry and Technology, Changsha 410004, China

**Jiaying He** – College of Materials Science and Engineering, Ministry of Forestry Bioethanol Research Center, and Hunan International Joint Laboratory of Woody Biomass Conversion, Central South University of Forestry and Technology, Changsha 410004, China

**Jin Liu** – College of Materials Science and Engineering, Ministry of Forestry Bioethanol Research Center, and Hunan International Joint Laboratory of Woody Biomass Conversion, Central South University of Forestry and Technology, Changsha 410004, China

Complete contact information is available at:

<https://pubs.acs.org/10.1021/acsomega.3c00927>

### Notes

The authors declare no competing financial interest.

## ACKNOWLEDGMENTS

This work was supported by the National Key Research and Development Program of the National Key Research and Development Program of China [2019YFE0114600], Key Research and Development Program of Hunan Province [grant 2020WK2019], and the Forestry Science and Technology Promotion Project [grant number [2019]22].

## REFERENCES

- (1) Chen, L. H.; Dou, J. Z.; Ma, Q. L.; Li, N.; Wu, R. C.; Bian, H. Y.; Yelle, D. J.; Vuorinen, T.; Fu, S. Y.; Pan, X. J.; et al. Rapid and near-complete dissolution of wood lignin at  $\leq 80$  °C by a recyclable acid hydrotrope. *Sci. Adv.* **2017**, *3*, No. e1701735.
- (2) Huang, D.; Li, R.; Xu, P.; Li, T.; Deng, R.; Chen, S.; Zhang, Q. The cornerstone of realizing lignin value-addition: Exploiting the native structure and properties of lignin by extraction methods. *Chem. Eng. J.* **2020**, *402*, No. 126237.
- (3) Alvira, P.; Tomas-Pejo, E.; Ballesteros, M.; Negro, M. Pretreatment technologies for an efficient bioethanol production process based on enzymatic hydrolysis: A review. *Bioresour. Technol.* **2010**, *101*, 4851–4861.
- (4) Watanabe, M.; Kanaguri, Y.; Smith, R. L. Hydrothermal separation of lignin from bark of Japanese cedar. *J. Supercrit. Fluids* **2018**, *133*, 696–703.
- (5) Ma, C. Y.; Xu, L.-H.; Zhang, C.; Guo, K.-N.; Yuan, T.-Q.; Wen, J.-L. A synergistic hydrothermal-deep eutectic solvent (DES) pretreatment for rapid fractionation and targeted valorization of hemicelluloses and cellulose from poplar wood. *Bioresour. Technol.* **2021**, *341*, No. 125828.
- (6) Yuan, T. Q.; Sun, S.-N.; Xu, F.; Sun, R.-C. Characterization of Lignin Structures and Lignin–Carbohydrate Complex (LCC) Linkages by Quantitative  $^{13}\text{C}$  and  $2\text{D}$  HSQC NMR Spectroscopy. *J. Agric. Food Chem.* **2011**, *59*, 10604–10614.
- (7) Feng, C. Q.; Zhu, J. T.; Hou, Y. J.; Qin, C. R.; Chen, W. Q.; Nong, Y. H.; Liao, Z. P.; Liang, C.; Bian, H. Y.; Yao, S. Q. Effect of temperature on simultaneous separation and extraction of hemicellulose using *p*-toluenesulfonic acid treatment at atmospheric pressure. *Bioresour. Technol.* **2022**, *348*, No. 126793.
- (8) Cai, C.; Hirth, K.; Gleisner, R.; Lou, H.; Qiu, X.; Zhu, J. Y. Maleic acid as a dicarboxylic acid hydrotrope for sustainable fractionation of wood at atmospheric pressure and  $\leq 100$  °C: mode and utility of lignin esterification. *Green Chem.* **2020**, *22*, 1605–1617.
- (9) Bian, H.; Chen, L.; Gleisner, R.; Dai, H.; Zhu, J. Y. Producing wood-based nanomaterials by rapid fractionation of wood at 80 °C using a recyclable acid hydrotrope. *Green Chem.* **2017**, *19*, 3370–3379.

- (10) Yang, M.; Gao, X.; Lan, M.; Dou, Y.; Zhang, X. Rapid Fractionation of Lignocellulosic Biomass by p-TsOH Pretreatment. *ENERGY FUELS* **2019**, *33*, 2258–2264.
- (11) Stanton, B. J.; Haiby, K.; Gantz, C.; Espinoza, J.; Shuren, R. A. The Economics of Rapid Multiplication of Hybrid Poplar Biomass Varieties. *FORESTS* **2019**, *10*, 446.
- (12) Zheng, A.; Jiang, L.; Zhao, Z.; Chang, S.; Huang, Z.; Zhao, K.; He, F.; Li, H. Effect of Hydrothermal Treatment on Chemical Structure and Pyrolysis Behavior of Eucalyptus Wood. *ENERGY FUELS* **2016**, *30*, 3057–3065.
- (13) Chen, C.; Chen, Z.; Chen, J.; Huang, J.; Li, H.; Sun, S.; Liu, X.; Wu, A.; Wang, B. Profiling of Chemical and Structural Composition of Lignocellulosic Biomasses in Tetraploid Rice Straw. *POLYMERS* **2020**, *12*, 340.
- (14) Ma, Y.; Li, H.; Yang, H.; Zhu, Y.; Zhao, L.; Li, M. Effects of solid acid and base catalysts on pyrolysis of rice straw and wheat straw biomass for hydrocarbon production. *J. Energy Inst.* **2022**, *101*, 140–148.
- (15) Sluiter, A.; Hames, B.; Ruiz, R.; Scarlata, C.; Sluiter, J.; Templaton, D.; Crocker, D. *Determination of structural carbohydrates and lignin in biomass, Technical Report NREL/TP-510-42618*, National Renewable Energy Laboratory, Golden, CO, 2010.
- (16) Zhu, J.; Chen, L.; Gleisner, R.; Zhu, J. Y. Co-production of bioethanol and furfural from poplar wood via low temperature ( $\leq 90$  °C) acid hydrolytic fractionation (AHF). *Fuel* **2019**, *254*, 115572.
- (17) Duan, Q.; Shuai, X.; Yang, D.; Zhou, X.; Gao, T. Kinetic Analysis of Pulping of Rice Straw with p-Toluene Sulfonic Acid. *ACS Omega* **2020**, *5*, 7787–7791.
- (18) Yao, S.; Nie, S.; Yuan, Y.; Wang, S.; Qin, C. Efficient extraction of bagasse hemicelluloses and characterization of solid remainder. *Bioresour. Technol.* **2015**, *185*, 21–27.
- (19) Majumdar, S.; Naha, A.; Bhattacharyya, D. K.; Bhowal, J. Effective delignification and decrystallization of cauliflower wastes by using dilute phosphoric acid for efficient enzymatic digestibility to produce fermentable sugars. *BIOMASS BIOENERGY* **2019**, *125*, 169–179.
- (20) Lan, T. Q.; Zheng, W. Q.; Dong, Y. F.; Jiang, Y. X.; Qin, Y. Y.; Yue, G. J.; Zhou, H. F. Exploring surface properties of substrate to understand the difference in enzymatic hydrolysis of sugarcane bagasse treated with dilute acid and sulfite. *Ind. Crops Prod.* **2020**, *145*, 112–128.
- (21) Wood, T. M.; Bhat, K. M. Methods for measuring cellulase activities. *Methods Enzymol.* **1988**, *160*, 87–112.
- (22) Yuan, X.; Wang, J.; Yao, H. Production of feruloyl oligosaccharides from wheat bran insoluble dietary fibre by xylanases from. *Food Chem.* **2006**, *95*, 484–492.
- (23) Jiang, H.; Chen, Q.; Ge, J.; Zhang, Y. Efficient extraction and characterization of polymeric hemicelluloses from hybrid poplar. *Carbohydr. Polym.* **2014**, *101*, 1005–1012.
- (24) Ci, Y. H.; Yu, F.; Zhou, C. X.; Mo, H. E.; Li, Z. Y.; Ma, Y. Q.; Zang, L. H. New ternary deep eutectic solvents for effective wheat straw deconstruction into its high-value utilization under near-neutral conditions. *Green Chem.* **2020**, 8713–8720.
- (25) Mounala Moukagni, E.; Ziegler-Devin, I.; Safou-Tchima, R.; Brosse, N. Extraction of acetylated glucuronoxylans and glucomannans from Okoume (*Aucoumea klaineana* Pierre) sapwood and heartwood by steam explosion. *Ind. Crops Prod.* **2021**, *166*, No. 113466.
- (26) Zhang, L.; Peng, W.; Wang, F.; Bao, H.; Zhan, P.; Chen, J.; Tong, Z. Fractionation and quantitative structural analysis of lignin from a lignocellulosic biorefinery process by gradient acid precipitation. *Fuel* **2022**, *309*, No. 122153.
- (27) Li, J.; Feng, P.; Xiu, H.; Li, J.; Yang, X.; Ma, F.; Li, X.; Zhang, X.; Kozliak, E.; Ji, Y. Morphological changes of lignin during separation of wheat straw components by the hydrothermal-ethanol method. *Bioresour. Technol.* **2019**, *294*, No. 122157.
- (28) Liu, J.; Liu, H.-F.; Deng, L.; Liao, B.; Guo, Q.-X. Improving aging resistance and mechanical properties of waterborne polyur-
- ethanes modified by lignin amines. *J. Appl. Polym. Sci.* **2013**, *130*, 1736–1742.
- (29) Dieste, A.; Clavijo, L.; Torres, A. I.; Barbe, S.; Oyarbide, I.; Bruno, L.; Cassella, F. Lignin from Eucalyptus spp. Kraft Black Liquor as Biofuel. *ENERGY FUELS* **2016**, *30*, 10494–10498.
- (30) Yang, X.; Li, Z.; Liu, H.; Ma, L.; Huang, X.; Cai, Z.; Xu, X.; Shang, S.; Song, Z. Cellulose-based polymeric emulsifier stabilized poly(N-vinylcaprolactam) hydrogel with temperature and pH responsiveness. *Int. J. Biol. Macromol.* **2020**, *143*, 190–199.
- (31) Gao, Y.; Guo, M.; Wang, D.; Zhao, D.; Wang, M. Advances in extraction, purification, structural characteristics and biological activities of hemicelluloses: A review. *Int. J. Biol. Macromol.* **2023**, *225*, 467–483.
- (32) Liu, L.; Chang, H. M.; Jameel, H.; Park, S. Furfural production from biomass pretreatment hydrolysate using vapor-releasing reactor system. *Bioresour. Technol.* **2018**, *252*, 165–171.
- (33) Wang, C. S.; Guo, J. J.; Hein, S.; Wang, H.; Zhao, Z. G.; Zeng, J. Foliar morphology and spatial distribution in five-year-old plantations of *Betula alnoides*. *For. Ecol. Manage.* **2019**, *432*, 514–521.
- (34) Wu, S.; Shen, D.; Hu, J.; Zhang, H.; Xiao, R. Role of  $\beta$ -O-4 glycosidic bond on thermal degradation of cellulose. *J. Anal. Appl. Pyrolysis* **2016**, *119*, 147–156.
- (35) Wan, C.; Zhang, G.; Zhang, F. A novel guanidine ammonium phosphate for preparation of a reactive durable flame retardant for cotton fabric. *Cellulose* **2020**, *27*, 3469–3483.
- (36) Kang, J.; Guo, Q.; Shi, Y.-C. NMR and methylation analysis of hemicellulose purified from corn bran. *Food Hydrocolloids* **2019**, *94*, 613–621.
- (37) Sun, S.-F.; Yang, H.-Y.; Yang, J.; Wang, D.-W.; Shi, Z.-J. Integrated treatment of perennial ryegrass: Structural characterization of hemicelluloses and improvement of enzymatic hydrolysis of cellulose. *Carbohydr. Polym.* **2021**, *254*, No. 117257.
- (38) Giummarella, N.; Lawoko, M. Structural Insights on Recalcitrance during Hydrothermal Hemicellulose Extraction from Wood. *ACS Sustainable Chem. Eng.* **2017**, *5*, 5156–5165.
- (39) Liu, W.-C.; Halley, P. J.; Gilbert, R. G. Mechanism of Degradation of Starch, a Highly Branched Polymer, during Extrusion. *Macromolecules* **2010**, *43*, 2855–2864.
- (40) Shi, Z.; Xu, G.; Deng, J.; Dong, M.; Murugadoss, V.; Liu, C.; Shao, Q.; Wu, S.; Guo, Z. Structural characterization of lignin from *D. sinicus* by FTIR and NMR techniques. *Green Chem. Lett. Rev.* **2019**, *12*, 235–243.
- (41) Ohra-aho, T.; Gomes, F. J. B.; Colodette, J. L.; Tamminen, T. S/G ratio and lignin structure among Eucalyptus hybrids determined by Py-GC/MS and nitrobenzene oxidation. *J. Anal. Appl. Pyrolysis* **2013**, *101*, 166–171.